Heat Transfer to a Liquid Fluidized Bed

ROBERT LEMLICH and ISIDORO CALDAS, JR.

University of Cincinnati, Cincinnati, Ohio

An experimental study of the rate of heat transfer from the retaining wall to a fluidized bed of solids was carried out for liquid water and glass spheres. The independent variables included mass velocity, particle size, bulk temperature, and wall temperature. Significant increases in heat transfer were observed, owing to the presence of the suspended solids, even to the extent of tripling the coefficient. For each of several particle sizes, the coefficient passed through a maximum corresponding to a particular mass velocity. The behavior of the bed at velocities below and above those for maximum coefficient was studied and categorized. Tentative correlations for both regions are offered.

Much work in recent years has dealt with heat transfer in fluidized beds. However, published data dealing with heat transfer from the retaining wall to the bed appear to be limited to systems wherein the fluid itself is a gas. Virtually nothing could be found for the case of a liquid. Accordingly, the present investigation was undertaken in an effort to study the transfer of heat from a vertical cylindrical retaining tube to a fluidized bed consisting of solid spheres suspended in water. The independent variables included mass velocity, particle diameter, wall temperature, and, to a lesser extent, bulk temperature and bed height.

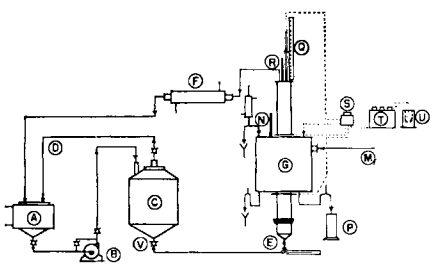

Fig. 1. Apparatus.

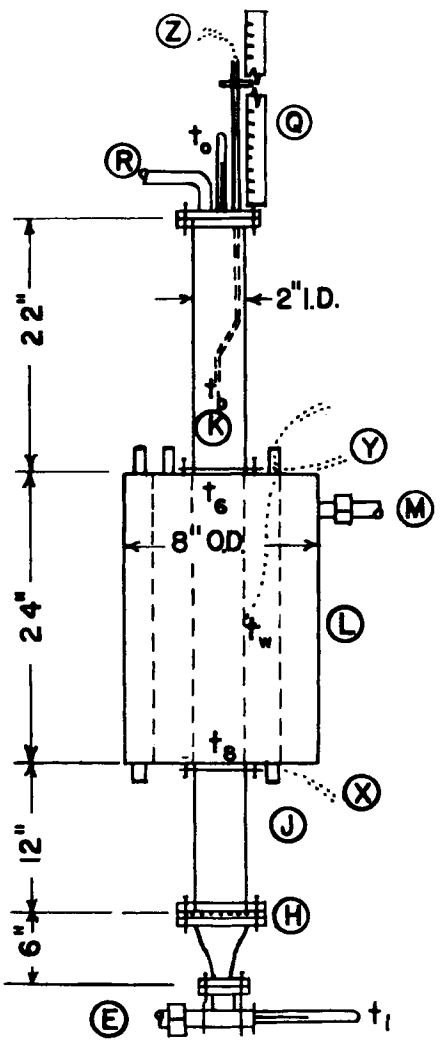

Fig. 2. Details of fluidizing unit.

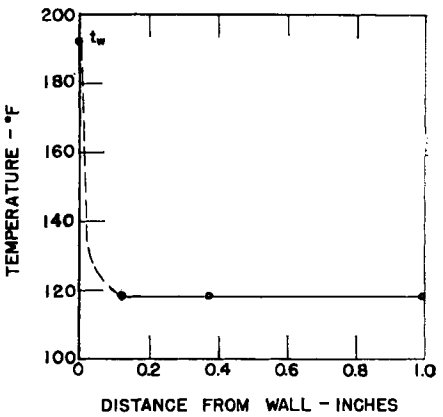

Fig. 3. Typical radial temperature profile in the fluidized bed.

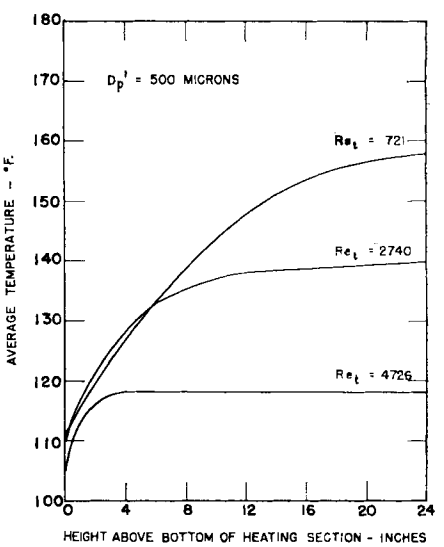

Fig. 4. Typical axial temperature profile in the fluidized bed.

EXPERIMENTAL

Materials

The solid particles employed were six closely sized groups of Scotchlite glass beads, ranging from 0.0019 to 0.027 in. in average diameter. Upon microscopic examination the beads appeared generally spherical with but little variation in diameter within any one group.

The diameter for each group was taken as the arithmetic mean of microscopic measurements on a representative sample of fifty to sixty beads from the particular group. The average diameters so obtained agreed closely with those specified by the manufacturer.

Absolute particle density for each bead size was determined by water displacement. Combining their value with bulk density measurements yielded an average value for the void fraction in the settled bed of about 0.43 with a standard deviation of about ±2% for all six bead sizes. Comparison with values offered by Brown (*1*) for randomly packed beds of solids indicates a sphericity of nearly unity, which is in accord with the high degree of sphericity observed microscopically.

The physical properties of the six groups of beads are summarized in Table 1.

Isidoro Caldas, Jr., is with Antibioticos S. A., Leon, Spain.

TABLE 1. PHYSICAL PROPERTIES OF GLASS BEADS

Average measured diameter, μ	Standard deviation in diameter, ±%	Particle density, lb./cu. ft. Absolute	Bulk
685	2.4	154	90
500	4.4	156	89
292	4.4	157	88
219	8.4	155	90
125	5.5	158	91
49	25	152	88

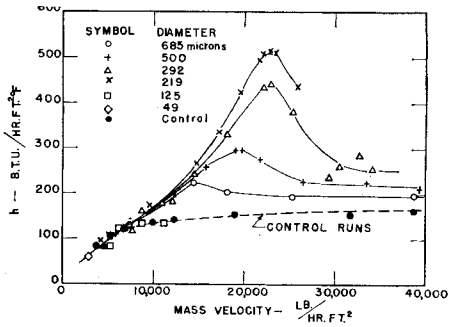

Fig. 5. Effect of flow rate and particle diameter on heat transfer coefficient, with steam as the heating medium.

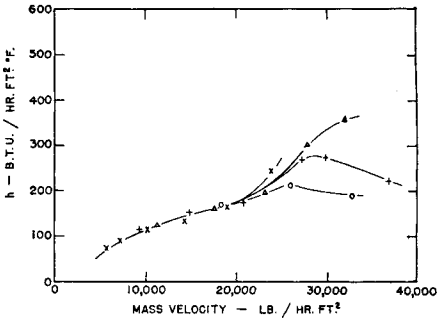

Fig. 7. Effect of flow rate and particle diameter on heat transfer. (Symbols are identified in Figure 5.)

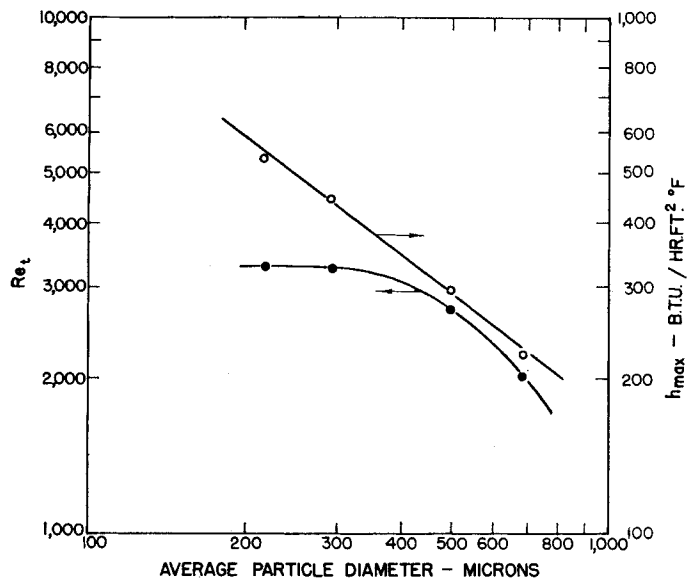

Fig. 6. Approximate transition between low- and high-velocity fluidization.

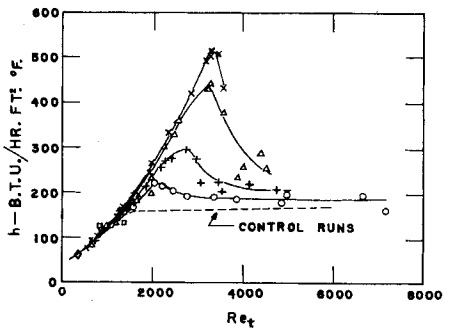

Fig. 8. Over-all results, showing effect of Reynolds number (based on tube diameter) and particle diameter on heat transfer coefficient. (Symbols are identified in Figure 5.)

The heating medium employed was a condensing vapor. For most of the work this was the general laboratory supply steam which was first passed through a moisture separator. For some runs, however, rectified methanol vapor was employed instead, in order to extend (downward) the temperature range.

Apparatus

An over-all schematic diagram of the equipment is shown in Figure 1. Distilled water from the jacketed circulating tank A was pumped B into the upper section of the ballast tank C. Any air entrapped in the liquid separated in this tank and escaped through the upper vent D. Water from the ballast tank under a slight positive pressure was admitted at a controlled rate to the bottom of the fluidizing column E passing upward through the bed of suspended solids and out through the water cooler F to the circulating tank.

The fluidizing unit itself G is a modification of that used by Dow and Jakob (*3*) in their work with air as the fluidizing medium. It is shown schematically in Figure 2. A 325-mesh copper screen H supported on a 40-mesh screen was used to support the bed of solids at the lower section of the column. A straight 1-ft. section of Pyrex-glass tubing J served as a straightening section and as a means for observing conditions in the lower part of the fluidized bed. A 2-ft. section of similar tubing K was used above the heating unit L and served as a disengaging section and as a means for observing the upper portion of the bed.

The heat transfer surface consisted of a 24-in.-long, 2-in.-I.D., 0.06-in.-thick copper tube surrounded by a double steam jacket. The outer steam jacket virtually eliminated any steam loss to the surroundings from the inner jacket. To further minimize heat losses, the entire unit was covered with asbestos paper and aluminum foil, except for narrow slits on the glass sections to permit visual observation. Vapor M was admitted at such a rate as to maintain a slight stream from the upper vent N. Condensate from each jacket was continuously drained P and collected separately.

Mercury thermometers measured the inlet water temperature t_i and the outlet water temperature t_0. A third thermometer measured the condensing vapor temperature. The wall temperature t_w was determined by means of a calibrated, glass-insulated, 20-gauge iron-constantan thermocouple welded in a groove approximately 1-in. long midway up the length of the copper heating tube. This groove was then filled with liquid solder and ground smooth and level with the rest of the condensing surface. Similar thermocouples X and Y were located at the center line of the inner tube at the entrance and exit to the heating section. In addition, a moving and rotatable thermocouple probe Z equipped with a calibrated scale Q was used to measure bed temperature t_b at various locations (to within ⅛ in. of the wall) and thus to determine longitudinal and radial temperature profiles throughout the fluidized bed. All thermocouples were connected via an ice-water cold junction U and a multiple contact switch S to a potentiometer, the precision of which was ±0.2°F.

Generally speaking, about 1½ to 2 hr. was required for the system to come to steady state after initial startup.

RESULTS

Control runs without solids, as well as fluidization runs with solids, were carried out. Detailed data and curves are available (*2*). At very low velocities some air bubbles appeared at the wall. Such runs were omitted.

Control Runs

Temperature-profile measurements for the control runs indicated virtually no radial variation in temperature at any level in the tube, even at Reynolds num-

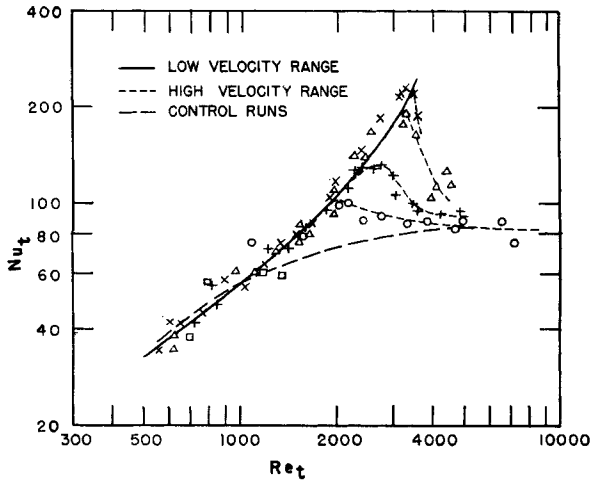

Fig. 9. Over-all results, showing relationship between Nusselt number and Reynolds number, both based on tube diameter. (Symbols are identified in Figure 5.)

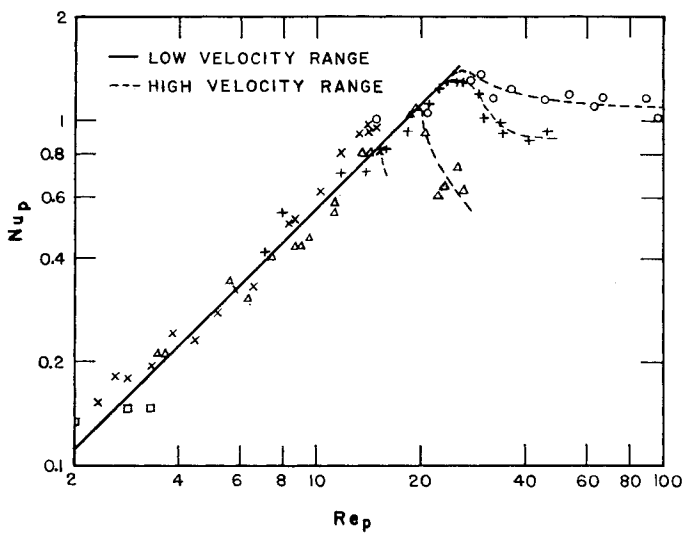

Fig. 10. Fluidation results, showing correlation for low-velocity regime. (Symbols are identified in Figure 5.)

bers Re_t (based on tube diameter) below 2,100. In other words, the temperature drop between wall and fluid was essentially confined to within $\frac{1}{8}$ in. of the wall. Furthermore, small quantities of ink introduced into the flowing stream at various levels were quickly dispersed, even at Re_t as low as 300 and with the walls unheated. This inherent mixing action is attributed to entrance effects and the relatively low ratio of tube length to diameter.

The heat transfer coefficient h for each run was computed from Equation (1). The quantity q was determined from the measured rise in temperature for a given rate of water flow. Comparison with q calculated from the measured rate of steam condensation from the inner jacket yields an average deviation of $\pm 5\%$, indicating a satisfactory heat balance.

$$h = \frac{q}{\int \Delta t \, dA} \qquad (1)$$

Table 2. Approximate Transition Between Low- and High-velocity Fluidization

Average particle diameter, μ	Reynolds number Based on tube diameter	Reynolds number Based on average particle diameter	Void fraction	Coefficient of heat transfer, B.t.u./(hr.)(sq. ft./°F.)	Increase in coefficient due to presence of particles, %
685	2020	27.3	0.542	224	57
500	2740	26.7	0.660	298	92
292	3260	18.8	0.816	442	178
219	3280	14.2	0.930	518	225

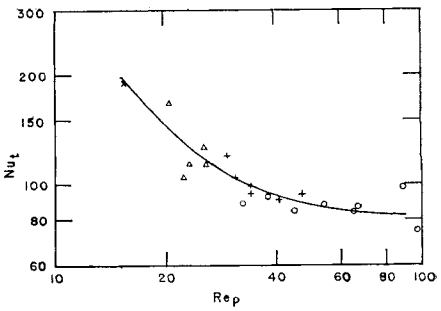

Fig. 11. Correlation for high-velocity regime. (Symbols are identified in Figure 5.)

The quantity $\int \Delta t \, dA$ was computed by graphical integration of the longitudinal profile. Results for the control runs are indicated as the broken curves in Figures 5 and 8. Some additional control runs (not shown), for which no temperature-profile measurements were taken but for which Δt was taken instead as constant at its arithmetic mean between inlet and outlet, were also carried out. The trend of these runs proved to be in fair agreement with the others.

Fluidization Runs

By and large little radial variation in temperature was observed for the runs with a fluidized bed. As with the control runs, radial variation in temperature appeared to be essentially confined to within $\frac{1}{8}$ in. of the wall, an indication that the major resistance to heat flow lies within this layer, in accordance with the usual film concept of resistance to convective heat transfer. A typical radial temperature profile is shown in Figure 3.

At high flow rates little longitudinal temperature variation was observed either, an indication of thorough mixing throughout the bed. Analogous results have been reported by others, such as Mickley and Trilling (*6*) in their work with air in the lean fluidization range. However, at lower flow rates longitudinal variation in temperature became pronounced, suggesting less vertical mixing. Figure 4 shows some longitudinal temperature profiles. Thus there are two general regimes, one for high flow rates and little vertical variation in temperature and a second for low flow rates and considerable vertical variation in temperature. In a limited sense, these two regimes may be considered analogous to lean and dense fluidization respectively in gas-solid systems. For the present liquid-solid system, the region of transition between the two regimes is, of course, not clearly defined; however, it does appear to be a function of particle size. It also falls in the usual Re_t transition range between viscous and turbulent flow.

Values for h were computed from

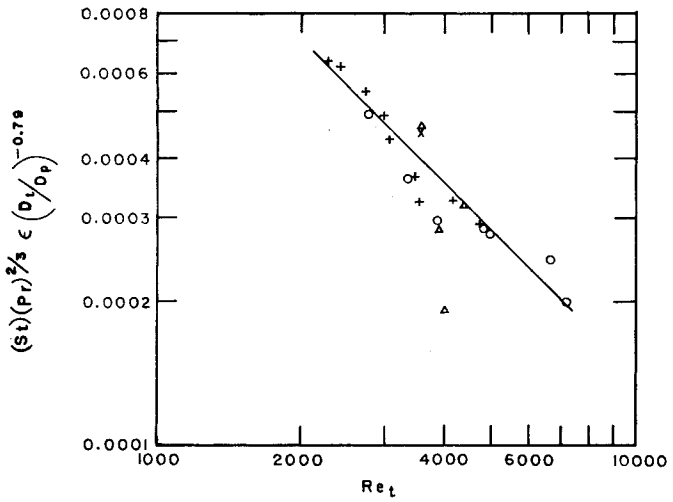

Fig. 12. Alternative correlation for high-velocity regime. (Symbols are identified in Figure 5.)

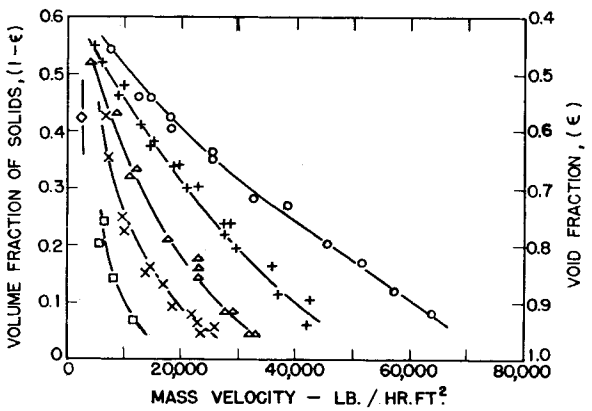

Fig. 13. Effect of mass velocity and particle size on solid fraction and void fraction. (Symbols are identified in Figure 5.)

Equation (1) and plotted against the mass velocity G in Figure 5 for runs with steam as the heating medium. The results show a marked improvement in h due to the presence of the fluidized particles, even to the extent of more than tripling the coefficient that would obtain in their absence. The maxima in h correspond approximately to the region of transition between these two regimes and are listed as such in Table 2. These maxima decrease with particle diameter as shown in Figure 6. (Carryover prevented attainment of sufficient mass velocity to yield a maximum h for the two smallest particle sizes of 49 and 125 μ. By the same token, the relatively sparse data obtained for these two smallest sizes are likely to be somewhat less reliable than the more extensive data taken for the four larger sizes.)

Maxima have been reported by others for gas-fluidized systems (*5*, *6*, *8*). Fitting this plot in Figure 6 with a straight line yields Equation (2) for the effect of particle diameter D_p' in microns on maximum h.

$$h_{max} = 34{,}400(D_p')^{-0.77} \qquad (2)$$

Similar results, shown in Figure 7, were obtained with condensing methanol as the heating medium. However, the corresponding curves are shifted downward and to the right as compared with those of Figure 5. By means of Re_t, both sets of data have been combined in Figure 8. Reasonable agreement is shown in this way between the data for the high-temperature levels of condensing steam and the data for the low-temperature levels of condensing methanol.

Improvement in h due to the presence of the solids in gas-fluidized systems has been ascribed (*7*) in part to the ability of the solids to carry heat. Compared to that of a gas under usual conditions, the volumetric heat capacity of a solid is very large; however, in the present work with water the volumetric heat capacity of the solid particles is actually less than half that of the fluid. Nevertheless, considerable increase in h has been obtained. It would thus appear likely that for liquid-fluidized systems, such as in the present investigation, convective transport by the solids is relatively slight and some other mechanism controls.

Low-velocity Fluidization

Figure 9 shows the effect of Re_t on Nu_t, the Nusselt number based on tube diameter, for all the data. Plotted in this way, all the results for the low-velocity regime cluster well about a common curve indicating the absence of any appreciable effect due to particle size. However, as the previously mentioned maximum h is approached, the results for the high-velocity regime appear to break away from the trend and to decrease along a different curve for each particle size. At the upper and lower extremes of Re_t the curve for the control runs is approached, and so extrapolation is possible at either end.

The analogous plot of Nusselt number based on particle size Nu_p vs. Reynolds number based on particle size Re_p is shown in Figure 10. As with the previous figure, the data for low-velocity fluidization follow a clear trend, while those for high-velocity fluidization branch off near the maximum. If the slight curvature in the low-velocity fluidization trend is disregarded, a straight line may be drawn through the data and fitted by the following simple equation:

$$Nu_p = 0.055Re_p \qquad (3)$$

No significant effect on h was found for the modest variation in bed height. Equation (3) fits the low-velocity fluidization data with a standard deviation of $\pm 13\%$. This relation can be readily transformed into Equation (4) where μ and k are the viscosity and thermal conductivity of the liquid respectively.

$$h = 0.055 \frac{k}{\mu} G \qquad (4)$$

Direct comparison with results of previous investigators, such as the recent correlation of Wen and Leva (*8*) for dense fluidization, is difficult, owing to the wide differences in physical properties between water and gases.

Thermal properties for these relationships are evaluated at the bulk temperature. Use of the arithmetic-mean film temperature did not appear to correlate the data any better.

High-velocity Fluidization

The data for high-velocity fluidization appear to scatter more than those for the low-velocity regime. Particle size has a definite effect, an increase in D_p' at constant G causing a decrease in h. Figure 11 shows Nu_t vs. Re_p, a method of plotting which allows for variation in particle size.

An alternative method of correlation is based on a modified Colburn-type j factor following an approach somewhat similar to that of Gamson (*4*). By a technique of successive cross plots, Figure 12 was prepared. Both particle size and void fraction ϵ are included here. A straight line was drawn and fitted by Equation (5)

$$j=(St)(Pr)^{\frac{2}{3}}=1.4(D_t/D_p)^{0.79}/Re_t\epsilon \quad (5)$$

All properties were evaluated at bulk temperature. The standard deviation for Equation (5) is ±19%. The effects of G and D_p' on ϵ are shown for both regimes in Figure 13. (Variation in temperature with attendant variation in fluid properties accounts for some of the scatter in this figure.)

SUMMARY OF CONCLUSIONS

1. The presence of fluidized solids can increase the rate of heat transfer from retaining wall to liquid considerably, a tripling of the coefficient having been obtained.
2. The behavior of the liquid-fluidized bed can be divided into two regimes, with the maximum coefficient for a given particle size occurring approximately at the transition.
3. The first regime at lower velocities is characterized by an appreciable vertical temperature gradient, which indicates limited axial mixing; by an increase of coefficient with mass velocity; and by a lack of any appreciable effect of particle size on coefficient. Within the limits of the experiment, results in this regime are correlated by Equations (3) or (4).
4. The second regime at higher velocities is characterized by little or no vertical temperature gradient, which is an indication of considerable axial mixing; by a decrease of coefficient with mass velocity; and by a decrease in coefficient with an increase in particle size. Within the limits of the experiment, results in this regime are correlated by Figure 11 or Equation (5).
5. In view of the low volumetric heat capacity of the solids in comparison with that of the liquid, it would appear that heat carried by the solids is not an important factor in determining the increase in heat transfer.

ACKNOWLEDGMENT

The authors wish to express their appreciation to Schenley Laboratories, Inc., of Lawrenceburg, Indiana, for the use of their facilities. The authors also thank William Licht and Chad Gottschlich for reviewing the original manuscript and Stuart Willins, Richard Lasure, and Chungkong Hwu for assistance in preparing the figures.

NOTATION

A = heat transfer surface, sq. ft.
c = heat capacity, B.t.u./(lb.)(°F.)
D = diameter, ft.
D' = diameter, μ
G = mass velocity, lb./(hr.)(sq. ft.)
h = coefficient of heat transfer, B.t.u./(hr.)(sq. ft.)(°F.)
k = thermal conductivity B.t.u./(hr.)(sq. ft.)(°F./ft.)
Nu = Nusselt number = hD/k, dimensionless
Pr = Prandtl number = $c\mu/k$, dimensionless
q = rate of heat transfer B.t.u./hr.
Re = Reynolds number = DG/μ, dimensionless
St = Stanton number = h/cG, dimensionless

Greek Letters

Δt = temperature difference, °F.
ϵ = void fraction, dimensionless
μ = viscosity, lb./(ft.)(hr.)

Subscripts

max. = maximum
p = particle
t = tube

LITERATURE CITED

1. Brown, G. G., "Unit Operations," p. 214, John Wiley and Sons, New York (1950).
2. Caldas, Isidoro, Ph.D. dissertation, Univ. Cinn. (1955), available from University Microfilms, Ann. Arbor, Mich.
3. Dow, W. M., and Max Jakob, *Chem. Eng. Progr.*, **47**, 637 (1951).
4. Gamson, B. W., *ibid.*, **47**, 19 (1951).
5. McAdams, W. H., "Heat Transmission," 3 ed., p. 303, McGraw-Hill Book Company, Inc., New York (1954).
6. Mickley, H. S., and C. A. Trilling, *Ind. Eng. Chem.*, **41**, 1135 (1949).
7. Van Heerden, C., A. P. P. Noble, and D. W. Van Krevelen, *Ind. Eng. Chem.*, **45**, 1237 (1953).
8. Wen, Chin-Yung, and Max Leva, *A.I.Ch.E. Journal*, **2**, 482 (1956).

COMMUNICATIONS TO THE EDITOR

Flow Measurement with Ball Flow Meters

H. L. SHULMAN and K. A. VAN WORMER, JR., Clarkson College of Technology, Potsdam, New York

The measurement of the rate of fluid flow is an essential part of control in almost all chemical plants. A wide variety of metering devices have been developed for this purpose ranging from relatively simple direct reading meters, such as the rotameter, to elaborate instrumentation for metering, recording, and controlling. Recently Gradishar (*2*) used a simple direct reading meter for gaseous hydrogen fluoride which avoided the difficulties encountered with the glass tubes used in rotameters. The reading meter consisted essentially of a section of Saran tubing in the shape of a quarter of a circle and a ball to serve as a quantitative indicator of the flow rate.

Shulman, Stieger, and Leist (*3*) modified this meter by employing a semicircular tube (Figure 1). This modification makes flow-rate measurements possible in either direction without the use of auxiliary valves and piping. In addition, the symmetry of the meter makes it possible easily to check the levelness of the installation because the ball should rest at the zero reading when there is no fluid flowing through the meter.

A ball flow meter can easily be constructed of a piece of transparent or translucent tubing and a ball which has a density greater than that of the fluid to be metered. If translucent tubing is employed, it should be mounted so that light may pass through it to facilitate locating the ball. Suitable tube materials include glass, vinyl, Tygon, Saran, and polyethylene. Balls can be metallic: steel, aluminum, and brass or nonmetallic: glass, nylon, sapphire, etc. The wide range of materials available and the ease of constructing this type of meter should make it very useful for laboratory, pilot plant, and exploratory work.

DERIVATION OF THE BALL-FLOW-METER EQUATION

For many applications ball flow meters can be calibrated experimentally with a trial-and-error procedure employed for the selection of the tube and ball. When toxic, corrosive, inflammable, or volatile fluids are to be metered, experimenta calibration is difficult or impossible. To aid in the selection of the tube and ball and in the prediction of calibration curves, an analytic and experimental study was undertaken to determine the factors influencing the design of ball flow meters.

An equation suitable for the prediction of calibration curves can be developed. When a fluid is flowing through the meter the ball comes to rest at a position indicative of the flow rate. This position is most conveniently measured by the angle which a radius of the circle extended through the center of the ball makes with the vertical (Figure 1). The ball remains in its position because there are two equal and opposite forces acting upon it. The first is the total drag of the fluid on the ball, which tends to move the ball up the tube. The second is the force due to the component of the weight of the ball which is acting parallel to the tangent at the point of contact of the ball and tube and which tends to move the ball down the tube. Goldstein (*1*) has

K. A. Van Wormer, Jr., is with Tufts University, Medford, Massachusetts.